

UNREALZOO: ENRICHING PHOTO-REALISTIC VIRTUAL WORLDS FOR EMBODIED AI AGENTS

Anonymous authors

Paper under double-blind review

ABSTRACT

The embodied artificial intelligence agents should be capable of sensing, reasoning, planning, and acting in complex open worlds, which are unstructured, high-dynamic, and uncertain. To apply agents in the real world, the realism of the simulated worlds is important for training and evaluating the built agents. This paper introduces UnrealZoo¹, a rich collection of photo-realistic 3D environments that mimic the complexity and variability of the real world based on Unreal Engine. For embodied AI, we provide a diverse array of playable entities in the environments and a suite of tools, based on UnrealCV, for data collection, reinforcement learning, and evaluation. In the experiments, we benchmark the agent on visual navigation and tracking, two fundamental tasks for embodied vision agents, in complex open worlds. The results provide valuable insights into the strengths of enriching the diversity of the training environments and the challenges to current embodied vision agents in the open worlds, e.g., the latency in the closed-loop control to interact with the dynamic objects, reasoning the accordance of the spatial structure in the complex scenes.

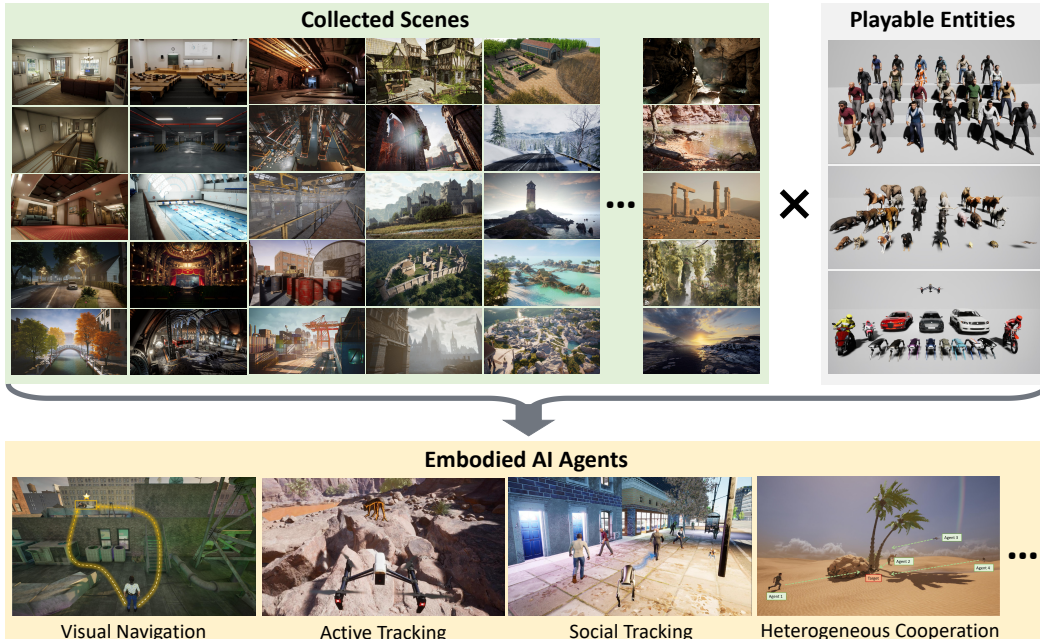


Figure 1: UnrealZoo enriches photo-realistic virtual worlds for embodied AI research by aggregating diverse scenes and playable entities. These environments facilitate the training and testing of embodied AI agents on tasks such as visual navigation, social tracking, and multi-agent cooperation, addressing challenges in open-world deployments.

¹Project page: <https://unrealzoo.notion.site/>

054 **1 INTRODUCTION**

055

056 Currently, embodied artificial intelligence (Embodied AI) agents are often *homebodies*, primarily
 057 confined to controlled indoor environments and rarely venturing outside to explore the diversity of
 058 the open world. While several simulators have advanced the field, including AI2-Thor (Kolve et al.,
 059 2017), OmniGibson (Li et al., 2023), VirtualHome (Puig et al., 2018), and Habitat (Puig et al., 2024),
 060 they often focus on specific scenarios, such as daily activities in homes, which limits the development
 061 of generalist embodied AI in open worlds. The lack of richness and variability in simulators hampers
 062 agents' ability to adapt and generalize to the diverse challenges of real-world environments, from
 063 bustling urban areas to rugged natural landscapes.

064 Thus, it is crucial to build diverse photo-realistic 3D virtual environments to simulate challenges in
 065 open worlds for advancing embodied AI. Such environments will help agents develop robust skills to
 066 sense, reason, plan, and control for accomplishing various tasks. By simulating complex scenarios and
 067 interactions, researchers can evaluate how embodied agents respond to uncertainty, adapt to dynamic
 068 challenges, and learn from their experiences in a controlled yet rich context. This process not only
 069 fosters the development of sophisticated perception and decision-making abilities but also enhances
 070 the agents' capacity to collaborate with humans and other AI systems, paving the way for seamless
 071 integration into real-world applications. As these virtual worlds grow increasingly sophisticated,
 072 incorporating realistic physics, intricate social dynamics, and varying levels of abstraction, they offer
 073 the potential for agents to experience a wider spectrum of situations. This diversity is essential for
 074 training robust agents that can generalize well to unseen environments and tasks. Furthermore, the
 075 iterative feedback loop between the agents and environments will enable continuous improvement,
 076 allowing agents to refine their skills through both simulated challenges and real-world encounters.

077 In this work, we introduce UnrealZoo, a comprehensive collection of photo-realistic virtual environ-
 078 ments set, based on Unreal Engine ² and UnrealCV (Qiu et al., 2017), featuring a diverse range of
 079 complex open worlds and playable entities to advance research in embodied AI. This high-quality
 080 set encompasses a wide range of complex indoor and outdoor scenes, such as houses, supermarkets,
 081 train stations, industrial factories, villages, temples, and natural landscapes, providing a platform
 082 to study how AI agents perceive and interact within a variety of complex dynamic environments.
 083 Each environment is carefully crafted by artists to replicate realistic lighting, textures, and dynamics,
 084 closely resembling real-world experiences. Our collection also includes diverse entities—humans, an-
 085 imals, robots, drones, motorbikes, and cars—each with unique appearances and movements, enabling
 086 researchers to investigate the generalization of the agents on different embodiments. To enhance
 087 usability, we have optimized UnrealCV and offer a suite of tools and APIs (UnrealCV+), including
 088 environment augmentation, demonstration collection, and distributed training/testing. These tools
 089 allow customization and extension of the environments to meet various research needs. This flexibility
 ensures UnrealZoo remains adaptable as the field of embodied AI evolves.

090 We conduct experiments to demonstrate the applicability of UnrealZoo for embodied AI. First,
 091 we benchmark frames per second (FPS) across various commands, highlighting the significant
 092 improvement in image rendering and multi-agent interactions with the UnrealCV+ API. We use
 093 embodied visual navigation and tracking as two example tasks to benchmark embodied vision agents
 094 in complex dynamic environments with moving objects and unstructured maps. We also introduce
 095 a set of simple yet effective baseline methods for developing embodied vision agents, including
 096 distributed online reinforcement learning algorithms, offline reinforcement learning algorithms, and a
 097 reasoning framework for large vision-language models (VLMs). Our evaluations across different
 098 settings emphasize the importance of diverse training environments for enhancing agent generalization
 099 and robustness, the necessity of low latency in closed-loop control to handle dynamic factors, and the
 potential of reinforcement learning for training agents to navigate complex scenes.

100 Our contributions can be summarized in the following: 1) We build UnrealZoo, a collection of
 101 100 high-quality photo-realistic scenes and a set of playable entities with diverse features, covering
 102 the most challenging to embodied AI agents in open worlds. 2) We optimize the communication
 103 efficiency of UnrealCV APIs and provide easy-to-use Gym interfaces with a toolkit for diverse
 104 requirements. 3) We conduct experiments to demonstrate the usability of UnrealZoo, showing the
 105 importance of the diversity of the environments to the embodied agents, and analyzing the limitations
 106 of the current RL-based and VLM-based agents in the open worlds.

107 ²www.unrealengine.com

108
 109
 110
 111
 112
 113 Table 1: The comparison with related photo-realistic virtual worlds for embodied AI. The comparison
 114 of visual realism across different engines is presented in Figure 6 and the emoji descriptions are
 115 listed in Table 6. (**Unstr. Terr.** indicating the presence of unstructured terrain. **Nav. Sys.** specifying
 116 whether the agent in the environment includes an autonomous navigation system.)
 117
 118
 119
 120

Virtual Worlds	Scene: Categories	Scene: Scale Level	Scene: Unstr. Terr.	Scene: Base Engine	Agent: Body	Agent: Nav. Sys.	Agent: Multi-agent
VirtualHome		Room	-	Unity		✓	✓
AI2THOR		Room	-	Unity		-	-
ThreeDWorld		Room, Building, Landscape	✓	Unity		-	✓
OmniGibson		Room	-	Omniverse	-	-	-
Habitat 3.0		Room	-	Habitat-Sim		✓	✓
CARLA		Building, Town	-	UE 4		-	✓
AirSim		Building, Town, Landscape	-	UE 4		-	✓
LEGENT		Room, Building	✓	Unity		✓	-
V-IRL		Town, Landscape	✓	Google Map		✓	✓
UnrealZoo		Room, Building, Town, Landscape	✓	UE 4/5		✓	✓

2 RELATED WORKS

123
 124
 125 **Realistic Simulators for Embodied AI.** Realistic simulators are extensively utilized in embodied
 126 artificial intelligence due to their appealing benefits, including high-quality rendering, cost-effective
 127 ground truth generation, low-cost interaction, and environmental controllability. They are crucial for
 128 training and testing AI agents to handle increasingly complex tasks. Notable realistic 3D simulators
 129 have been created for specific applications, such as indoor navigation (Kolve et al., 2017; Puig et al.,
 130 2018; Xia et al., 2018; Wu et al., 2018), robot manipulation (Yu et al., 2020; Ehsani et al., 2021;
 131 Chen et al., 2024), and autonomous driving (Gaidon et al., 2016; Shah et al., 2018; Dosovitskiy
 132 et al., 2017). Recent advances in computer graphics have spurred interest in developing general-
 133 purpose virtual worlds with photo-realistic rendering, allowing agents to collect high-fidelity data
 134 and learn skills applicable across various tasks and scenes. ThreeDWorlDs (TDW) (Gan et al., 2021)
 135 and LEGENT (Cheng et al., 2024) are notable simulators that offer photo-realistic, multi-modal
 136 platforms, based on Unity, for interactive physical simulation. However, their built-in scenes and
 137 playable entities are somewhat limited. Additionally, the performance of the simulator decreases
 138 significantly in large outdoor environments, a typical weakness of Unity. V-IRL (Yang et al., 2024)
 139 is a recent approach that leverages Google Maps’ API to simulate agents with real-world street
 140 view images, significantly reducing the gap between virtual and real-world settings. However, since
 141 V-IRL is inherently composed of static images, it lacks the capability to simulate the dynamics of the
 142 physical worlds for agent-object interactions. Recently, the community has also begun to explore
 143 dynamic environments with social interactions and unexpected events. However, existing solutions
 144 like Habitat 3.0 (Puig et al., 2024) focus on a limited number of agent interactions in indoor scenes,
 145 while HAZARD (Zhou et al., 2024b) addresses only single-agent simulations in dynamic scenarios
 146 like fires, floods, and winds. In contrast, UnrealZoo offers a comprehensive collection of scenes
 147 that feature dynamic situations and diverse playable entities for embodied AI. With advancements
 148 in Unreal Engine and optimized UnrealCV, our environment achieves real-time performance in
 149 large-scale scenes with multiple agents (around 10) and photo-realistic rendering. A comprehensive
 150 comparison across the related photo-realistic simulators is shown in Table 1.
 151

152 **Embodied Vision Agents.** Embodied vision agents, which perceive and interact with their envi-
 153 ronments through vision, are a key focus in artificial intelligence research. These agents perform
 154 tasks like navigation (Zhu et al., 2017; Gupta et al., 2017; Yokoyama et al., 2024; Long et al., 2024),
 155 active object tracking (Luo et al., 2018; Zhong et al., 2019; 2021; 2023; 2024), and other interactive
 156 tasks (Chaplot et al., 2020; Weihs et al., 2021; Ci et al., 2023; Wang et al., 2023), mimicking human
 157 behavior. Their development involves various methods, including state representation learning (Ya-
 158 dav et al., 2023; Yuan et al., 2022; Gadre et al., 2022; Yang et al., 2023), reinforcement learning
 159 (RL) (Schulman et al., 2017; Xu et al., 2024; Ma et al., 2024), and large vision-language models
 160 (VLMs) (Zhang et al., 2024; Zhou et al., 2024a). Despite significant progress, challenges remain.
 161 RL methods often require extensive trial-and-error interactions and computational resources for training,
 162 and they usually struggle to generalize to new environments. Conversely, VLM-based methods excel
 163 at interpreting language instructions and images but may lack the fine-grained control and adaptability
 164 necessary for real-time interactions. The computational demands and time needed for inference with
 165 such large models are critical, especially in dynamic scenes. Moreover, previous simulators mainly

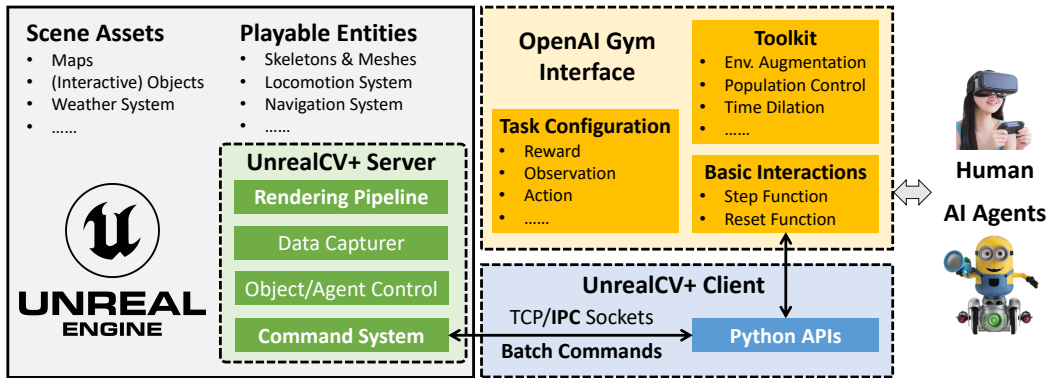


Figure 2: The detailed architecture of UnrealZoo. The Gray box indicates the UE binary, collecting the scenes and playable entities. The UnrealCV+ Server is built in the binary as a plugin. We have bolded the names of the optimized or new modules in UnrealCV+ Server and Client. For agent-environment interaction, we provide OpenAI Gym Interface, which has been widely used in the community. Our gym interface supports customizing the task in a configuration file and contains a toolkit with a set of gym wrappers for environment augmentation, population control, etc.

focus on indoor rooms or urban roads, which mask the potential challenges to the embodied agents when deploying in open worlds, e.g., unstructured terrain, dynamic changing factors, inference costs of the perception-control loop, and social interactions with other agents. Therefore, it is required to benchmark agents in large-scale, photo-realistic open worlds, taking into account various real-world challenges in the virtual worlds. In this work, we collect a subset of environments from UnrealZoo and benchmark embodied visual navigation and tracking agents, to emphasize the weakness of the existing methods.

3 UNREALZOO

UnrealZoo is a collection of photo-realistic, interactive open-world environments with diverse embodied characters, built on Unreal Engine and UnrealCV (Qiu et al., 2017). The environments are sourced from the *Unreal Engine Marketplace*³, which shares 3D resources from artists, and were accumulated over two years at a cost exceeding 10,000. UnrealZoo features a diverse array of scenes with varying sizes and styles. Among them, the largest scene, i.e., Medieval Nature Environment, covers more than 16km^2 areas. The environments also include a wide range of embodiment, such as human avatars, vehicles, drones, animals, and virtual cameras, all of which can interact with the environment and equipped with ego-centric sensing systems. We offer easy-to-use Python APIs based on UnrealCV to facilitate interaction between Python programs and the game engine. Note that UnrealCV is optimized for rendering and communication, particularly in large-scale and multi-agent scenarios, namely UnrealCV+. Additionally, we provide OpenAI Gym interfaces to standardize agent-environment interactions. The gym-like interface also contains a set of toolkits, e.g., environment augmentation, population control, time dilation, and JSON-style task configurations to help the user customize the environments for various tasks with minimal effort. The project website includes the details of the collected contents, and documents about tutorials, Python APIs, and the gym interface.

3.1 SCENE COLLECTION

UnrealCV Zoo contains 100 scenes based on Unreal Engine 4 and 5. We select the scene based on the public reviews in the marketplace and the difference to the collected scenes, aiming at covering a wide range of styles from realistic to fictional, ensuring diversity. We provide an overview of the environments in the scene gallery.

³<https://www.unrealengine.com/marketplace>

We have tagged the collected scenes with a number of feature labels allowing researchers to select appropriate scenes for testing or training based on the tags associated with each scene. Our tags cover the following aspects:

- Scene Categories:** We categorize scenes into three main types: interior, exterior, and both. The interiors include private houses, museums, supermarkets, train stations, factories, gyms, and caves. The exteriors include various outdoor terrains such as ruins, islands, plazas, neighborhoods, and mountains. Additionally, there are 25 scenes that feature both interior and exterior features, requiring enhanced spatial reasoning to comprehend their structure.
- Spatial Structure:** We also tag the spatial structure of the scenes, including multi-floor, topological, flat, steep, etc. Such categorization is vital for benchmarking embodied agents, where the agent's performance is greatly impacted by the geometric structures.
- Dynamics:** Environments featuring significant weather and animation change that create random dynamic lighting variations, visual obstructions, and effects such as sandstorms, snowfall, and thunderstorms, enhancing the environment's interference with visual tasks. Besides, we also label the environments with *interactive objects* where agents can interact with objects, e.g., open a door. These dynamics are essential for the open world.
- Scale:** Each scene is labeled by the scale, such as small (room-level), medium (building-level), and large (city-level or landscape-level). Extra-large maps with delicate buildings, terrain, and illumination, are available for complex, long-term tasks such as rescues, which require extensive environments and high exploration needs.
- Style:** The scenes may also reflect different cultural backgrounds, such as *Asian Temple*, *Western Church*, *Middle East Street*, or *Modern City*, *Science Fiction*. Identifying cultural styles will help us build a new data set to benchmark how social agents adapt to diverse cultures and social norms.

After categorizing the scenes, we integrate UnrealCV+ into the UE project (Refer to Section 3.3) and add the controllable player assets (Refer to Section 3.2) to each scene. Due to licensing restrictions, content purchased from the marketplace cannot be open-source, so we will package the projects into an executable binary for sharing with the community. These executable binaries will be compatible with various operating systems, including Windows and Linux, allowing users to download and run them via the Python interface without needing any knowledge of Unreal Engine, which is primarily built on C++ and Blueprint.

3.2 PLAYABLE ENTITIES

UnrealZoo includes seven types of entities: humans, animals, cars, motorbikes, drones, mobile robots, and flying cameras (See Figure 1). Specifically, it comprises 19 human entities, 27 animal entities, 3 cars, 14 quadruped robots, 3 motorcycles, and 1 quadcopter drone. This diversity, with varying affordances like action space and viewpoint, allows us to explore new challenges in embodied AI, such as cross-embodiment generalization and heterogeneous multi-agent interactions.

Each entity includes a skeleton with appropriate meshes and textures, a local motion system, and a navigation system. We offer a set of callable functions for each entity, enabling users to modify attributes like size, appearance, and camera positions, as well as control movements. Each entity can switch between different textures and appearances via UnrealCV API, enhancing visual diversity

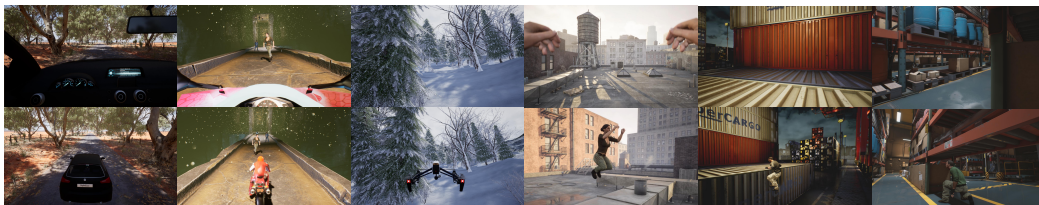


Figure 3: The first-person view images (Top) while playing different entities and motions across various scenes.

270 Table 2: Comparison of FPS in Unreal Engine 4.27 with UnrealCV and UnrealCV+.
271

	Image Capture				Multi-agent Interaction		
	Color	Obj. Mask	Suf.	NorDepth	N=2	N=6	N=10
UnrealCV	74	70	109	52	35	13	8
UnrealCV+	83(↑ 12%)	154(↑ 120%)	131(↑ 20%)	97(↑ 86%)	54(↑ 54%)	25(↑ 92%)	16(↑ 100%)

272 and adaptability for various scenarios. Each entity is equipped with an ego-centric camera, allowing
273 researchers to capture various types of image data such as RGB, depth, surface normal, and instance-
274 level segmentation from the agent’s ego-centric view. Figure 3 shows examples of the captured
275 first-person view and third-person view images of different entities with varying locomotion. For
276 multi-agent interaction, the population of the entities in a scene can be easily adjusted using the
277 spawn or destroy functions.

278 **The locomotion system** is built on Smart Locomotion, a well-designed and smooth locomotion
279 system. It contains a number of high-quality animations that enable the agent to interact with
280 the scene, such as opening and closing doors, crouching under obstacles, jumping over obstacles,
281 climbing onto a platform, and simulating injury or death. With the locomotion system, we can explore
282 the agent’s ability to reason, plan, and interact in large-scale complex 3D scenes in advance, ignoring
283 learning skills for low-level action control that requires high-fidelity physical simulation.

284 **The navigation system** is built on NavMesh allowing agents to autonomously navigate with the built-
285 in AI controller in the Unreal Engine. This includes path-finding and obstacle-avoidance capabilities,
286 ensuring smooth and realistic movement throughout diverse terrains and structures. For urban-style
287 maps, we segment the roads to distinguish between pedestrian and vehicle pathways. When agents
288 use the navigation system for autonomous control, they will navigate the shortest path based on
289 the priority of the different areas. For example, pedestrians and animals will prioritize walking on
290 sidewalks, while vehicles and motorcycles will prioritize driving on roadways. An example of the
291 navigation area is shown in Figure 9.

292 3.3 PROGRAMMING INTERFACE

293 We provide UnrealCV+ as the basic application programming interface (API) on Python to capture
294 data and control the entities and scenes, and provide an OpenAI Gym interface for general agent-
295 environment interactions. The architectures of the programming interfaces are shown in Figure 2.

296 **UnrealCV+** is our modification version of the UnrealCV (Qiu et al., 2017) for high-throughput
297 interactions. As the original version of UrnealCV primarily focuses on data generation, the frame rates
298 per second (FPS) are not optimized for real-time interactions. We optimize the rendering pipelines
299 in UnrealCV Server and the communication protocols between UnrealCV Server and Client to
300 improve the FPS. Specifically, we enable parallel processing while rendering object masks and depth
301 images, which can significantly improve the FPS in large-scale scenes. For multi-agent interactions,
302 we further introduce the batch commands protocol. In this protocol, the client can simultaneously
303 send a batch of commands to the server, which can process all the received commands and return a
304 batch of results. In this way, we can reduce the time spent on server-client communication. Since
305 reinforcement learning requires an extensive number of trial-and-error interactions for training, often
306 running multiple environments on a computer, we additionally introduce Inter-process communication
307 (IPC) sockets instead of the TCP sockets to improve the stability of the server-client communication
308 under high loads. We benchmark the FPS performance in Table 2. To enhance user-friendliness, we
309 have developed high-level Python APIs that are built upon the command systems of UnrealCV. These
310 APIs encapsulate all the request commands and their corresponding data decoders into a callable
311 Python function. This approach significantly simplifies the process for beginners, allowing them to
312 interact with and customize the environment using UnrealCV+.

313 **OpenAI Gym Interface** is used to define the tasks and standardize the agent-environment interaction,
314 following Gym-UnrealCV. Even though there are a lot of tasks for agents, they usually share common
315 interaction protocols, i.e., the agent gets observations from the environment and returns actions. The
316 main difference across different tasks usually is the reward functions, the modality of the observation,
317 and the available actions. Hence, we define the basic interaction functions for general usage and list
318 the task-specific configurations, e.g., scene name, and reward function, in a JSON File, as shown in
319 Figure 11. In this way, when adding new UE scenes, the users only need to set the parameters in the
320

324 JSON files. Moreover, we contain a toolkit with a set of gym wrappers for training and testing the
 325 agents, such as environment augmentation that has been in previous work for training generalizable
 326 agents (Luo et al., 2018; 2020), population control to adjust the number of agents in the scene, and
 327 time dilation to adjust the control frequency in dynamic scenes. In Section 4.3, we demonstrate an
 328 example usage of the toolkit to analyze the robustness of social tracking agents to the population of
 329 crowds and the impact of the control frequency in such dynamic scenes. We also provide a launch
 330 tool to enable the user to run multiple environments with specific GPU IDs within a computer, which
 331 is useful for distributed online reinforcement learning.

332 4 EXPERIMENTS

333 In this section, we use a subset of UnrealZoo to demonstrate the usability of the collected environments.
 334 For visual navigation, we select two scenes with complex spatial structures to train and validate
 335 the RL-based and VLM-based agents. For active tracking, we select at most 8 scenes as training
 336 environments and validate the generalization of the learned policy in another 24 scenes, which are
 337 divided into four categories according to the scene types. The results demonstrate the importance of
 338 the diversity of the training environments to the cross-domain generalization. For social tracking, we
 339 analyze the robustness of the agent in social environments with different control frequencies, using
 340 the toolkit provided in the gym to generate crowds with varying populations and control frequencies.
 341

342 4.1 VISUAL NAVIGATION

343 In-the-wild visual navigation introduces a new level of complexity compared to traditional navigation
 344 tasks for indoor scenes or autonomous driving, which often run on structured maps. Differently, we
 345 place the agent in open-world environments where it must take a set of locomotions, e.g., running,
 346 climbing, jumping, crouching, to go over the various obstacles in unstructured terrains to reach the
 347 target object. In this setting, the agent requires advanced scene reasoning and action affordance to
 348 make real-time decisions about its path. The emphasis on such complex environments ensures the
 349 agent can operate effectively in a broad range of challenging scenarios, moving beyond the constraints
 350 of traditional navigation frameworks. The details of the task setting are introduced in Appendix B.1.
 351

352 **Evaluation Metrics.** We employ two key metrics to evaluate visual navigation agents: 1) Average
 353 Episode Length (EL), representing the average number of steps per episode over 50 episodes. 2)
 354 Success Rate (SR), measuring the percentage of episodes the agent successfully navigates to the target
 355 object out of 50 total episodes, which represents the navigation capability in the wild environment.

356 **Baselines for Navigation.** We build simple baselines to demonstrate the applicability of our envi-
 357 ronments for training reinforcement learning agents and benchmark the agents based on pre-trained
 358 large models. **1) Online RL:** We trained the RL-based navigation agents separately in the Roof
 359 and Factory environments using a distributed online reinforcement learning (RL) approach, e.g.
 360 A3C (Mnih et al., 2016). The training curve is shown in Figure 15. The model takes the first-person
 361 view segmentation mask and the relative position between the agent and target as input, and outputs
 362 direct control signals (from the predefined action space) to navigate. This setup allows the agent to
 363 learn and optimize navigation strategies during continuous interaction with the environment. Please
 364 refer to Appendix C.1 for the implementation details. **2) GPT-4o:** We employ the GPT-4o model to
 365 take action, leveraging its powerful multi-modal reasoning capabilities. The model takes first-person
 366 view images and the relative position between the agent and the fixed target as input. The GPT-4o
 367 model follows our prompt template (See Table 13) as guidance, reasoning appropriate actions from
 368 the predefined control space to guide the agent toward the target. **3) Human:** We also have a human
 369 player control the agent using a keyboard, similar to a first-person video game. The player navigates
 370 the agent from a random starting point to a fixed target, making decisions based on visual observations
 from the shared control space.

371 **Results.** In Table 3, we report the performances of different methods in two unstructured scenes.
 372 The RL-based agent performs moderately well, achieving better results in the simpler IndustrialArea
 373 environment compared to the Roof environment, where the target object is located on different levels
 374 of stairs. The agent based on GPT-4o struggles in both scenarios. This infers that the GPT-4o performs
 375 poorly in complex 3D scene reasoning. As a reference, the human player completes both tasks with
 376 the fewest steps and a 1.00 success rate, underscoring the significant gap between current embodied
 377 AI agents and human performance, indicating substantial room for improvement to navigate in such
 complex, open-world environments.

Figure 4: An exemplar sequence from the RL-based agent in the *Roof*.

4.2 ACTIVE VISUAL TRACKING

We evaluate the generalization of the tracking agents across four environment categories: **Interior Scenes, Palaces, Wilds, and Modern Scenes**. Each category contains 4 individual environments, as shown in Figure 8. We aim to capture a broad range of features in our environment collection by selecting four distinct and representative scenes from each category, ensuring a comprehensive evaluation of the agents’ capabilities. The details of the tasks are introduced in Appendix B.2. We analyzed the effectiveness of the diversity of the training data by collecting demonstrations with different numbers of training environments.

Evaluation Metrics. Our evaluation employs three key metrics: (1) Average Episodic Return (ER), which calculates the mean episodic return over 50 episodes, providing insights into overall tracking performance; (2) Average Episode Length (EL), representing the average number of steps per episode, which reflects long-term tracking effectiveness; and (3) Success Rate (SR), measuring the percentage of episodes that complete 500 steps out of 50 total episodes.

Baselines for Active Tracking. For the *RL-based agents*, we extend from the official implementation settings from the recent offline RL method (Zhong et al., 2024), collecting offline datasets and employing the original network architecture. To demonstrate the impact of data diversity on tracking performance, we collect three sets of offline datasets, each containing 100k steps. The key difference between these datasets is the number of environments used for data collection: one was collected in a single environment (denoted as *1 Env.*), another in two environments (denoted as *2 Envs.*), and the third in eight distinct environments (denoted as *8 Envs.*). The offline training curve of each setting is shown in Figure 14. The environment distribution of each dataset setting is shown in Figure 10. It is worth noting that *FlexibleRoom*, one of the environments used for data collection, is a unique abstract environment, with all objects represented as geometric shapes covered by randomized patterns. This distinctive setup contrasts with the more realistic and diverse environments in the collection, offering a unique scenario for testing agent adaptability. For the *VLM-based agents*, we utilize the latest large models GPT-4o to directly generate actions based on observed images for tracking a target person. To ensure smooth and precise transitions, we designed a system prompt that helps the model understand the task while standardizing the output format to align with predefined action settings. This prompt ensures the model produces actions coherent with the task’s requirements. Specifically, GPT-4o is tasked with generating concrete action decisions from a predefined instruction space: moving forward, moving backward, turning left, turning right, or maintaining the current position. Once an instruction is generated, we map it to corresponding linear and angular velocities to update the agent’s movement in the environment. It is important to note that while the system prompt can use raw image observations as input, our experience shows poor alignment performance and significant time delays, which pose challenges for real-time tracking. The full system prompt and mapping relationship are provided in Appendix C.2.

Result Analysis. We first evaluate the performance of agents trained with offline datasets collected from varying numbers of environments (1 Env., 2 Envs., 8 Envs.) across **16 distinct environments**. We list the detailed evaluation results across the entire 16 environments in Table 11. To better visualize

Table 3: The results (EL/SR) of in-the-wild visual navigation in two unstructured terrains.

Methods	Roof	IndustrialArea
Online RL	1660/0.32	261/0.52
GPT-4o	2000/0.00	369/0.20
Human	515/1.00	158/1.00

the performance change of different training settings within various scene categories, we calculate the average success rate (SR) of each agent in four categories, the results are shown in Figure 5. The results reveal a clear trend: **as the number of environments used for training increases, agent long-term tracking performance generally improves across all categories.** In the Wilds, a significant increase in success rate is observed with the 8 Envs. dataset, which involves the highest diversity of environments. This demonstrates that diverse environmental exposure plays a crucial role in improving the agent’s generalization capabilities in more complex, open-world environments. The lower success rate in the 1 Env. dataset highlights the limitations of training solely in abstract settings like the FlexibleRoom. Similarly, in the Palace, the success rate improves notably from 1 Env. to 8 Envs., suggesting that training with a broader range of environments helps the agent better adapt to intricate spatial structures typical of Palace-like maze environments.

4.3 SOCIAL TRACKING

We further evaluate the tracking agents in a social tracking setting, where the agent needs to follow the target in crowds. Such a setting contains varying high-dynamics objects with similar appearances. We can directly apply the toolkit provided in the Gym interface to extend the *DowntownWest* environment used for active tracking to this setting.

Robustness to Active Distractions. A key challenge in active visual tracking tasks is managing active distractions, a critical issue for real-world deployment in crowds. Thus, we conducted an experiment in the *DowntownWest* environment and generated crowds with varying numbers of human characters as distractors notated as 4D, 8D, and 10D. We compared the performance of the offline RL method, trained under three dataset configurations (1 Env., 2 Envs., 8 Envs.), against the VLM-based method, evaluating the agents’ ability to maintain robust tracking under these different levels of active distractions. The results in Table 5 show clear performance differences between the offline RL methods (1 Env., 2 Envs., 8 Envs.) and the GPT-4o model in handling active distractions. As the number of distractors increases, the offline RL methods maintain relatively stable success rates (SR), with the highest performance seen in the 8 Envs. setting, which achieves an SR of 0.8 in the 4D condition and remains robust with slight declines in the 8D and 10D conditions (0.72 and 0.68, respectively). This suggests that the agent benefits from the richer diversity of training data, enabling it to handle increasingly complex crowd scenarios more effectively. On the other hand, the GPT-4o model consistently struggles with active distractions, showing significantly lower average returns (ER) and success rates across all settings. The model’s inability to cope with dynamic, crowded environments is evidenced by its poor performance, particularly in the 10D condition where it records a success rate of just 0.1. This highlights a major limitation of the VLM-based method in dynamic environments with active distractions, as it lacks the temporal consistency and real-time adaptability required for effective tracking.

Cross-Embodiment Generalization. We transfer the agent trained for the human character to the robot dog, which observes the world from a lower perspective. We can see that the results in Table 5 drop, particularly the success rate, indicating that the research community should pay more attention to the cross-embodiment generalization.

The Impact of Control Frequency. We employ the time dilation wrapper to simulate different control frequencies during deployment. The frequency of the perception-control loop is crucial for handling dynamic environments. As is shown in Table 4, when the rate drops below 10 FPS, performance significantly declines. We observe that higher control frequencies enable RL-based

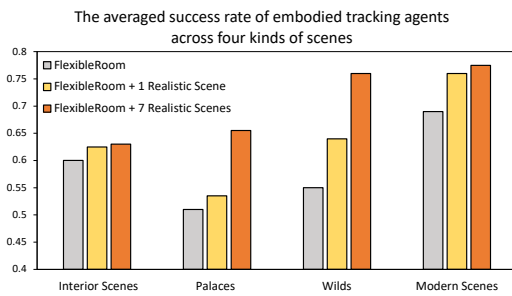


Figure 5: Average success rate of agents across four environment categories: Compact Interior, Wildscape Realm, Palace Maze, and Lifelike Urbanity, evaluated under three offline dataset settings (1 Env., 2 Envs., 8 Envs.). The results show the generalization capability improves significantly as more diverse environments are included in the dataset. However, environments with complex spatial structures, such as Compact Interior and Palace Maze, exhibit lower success rates, highlighting challenges in obstacle avoidance and navigation.

success rates. As the number of distractors increases, the offline RL methods maintain relatively stable success rates (SR), with the highest performance seen in the 8 Envs. setting, which achieves an SR of 0.8 in the 4D condition and remains robust with slight declines in the 8D and 10D conditions (0.72 and 0.68, respectively). This suggests that the agent benefits from the richer diversity of training data, enabling it to handle increasingly complex crowd scenarios more effectively. On the other hand, the GPT-4o model consistently struggles with active distractions, showing significantly lower average returns (ER) and success rates across all settings. The model’s inability to cope with dynamic, crowded environments is evidenced by its poor performance, particularly in the 10D condition where it records a success rate of just 0.1. This highlights a major limitation of the VLM-based method in dynamic environments with active distractions, as it lacks the temporal consistency and real-time adaptability required for effective tracking.

Cross-Embodiment Generalization. We transfer the agent trained for the human character to the robot dog, which observes the world from a lower perspective. We can see that the results in Table 5 drop, particularly the success rate, indicating that the research community should pay more attention to the cross-embodiment generalization.

The Impact of Control Frequency. We employ the time dilation wrapper to simulate different control frequencies during deployment. The frequency of the perception-control loop is crucial for handling dynamic environments. As is shown in Table 4, when the rate drops below 10 FPS, performance significantly declines. We observe that higher control frequencies enable RL-based

486
 487 Table 5: Performance comparison of different methods in the DowntownWest environment with
 488 varying numbers of distractors (4D, 8D, 10D). Each cell presents three metrics from left to right:
 489 Average Episodic Return (ER), Average Episode Length (EL), and Success Rate (SR).

Method	4D	8D	10D
Offline RL 1 Env.	251/450/0.70	201/406/0.58	230/247/0.64
Offline RL 2 Envs.	309/456/0.74	259/424/0.68	258/428/0.68
Offline RL 8 Envs.	245/458/0.80	225/435/0.72	218/444/0.68
Offline RL 8 Envs. (Robot dog)	220/409/0.48	189/386/0.42	143/367/0.40
GPT-4o	-102/264/0.16	-64/270/0.14	-80/240/0.10

496 agents to perform better in social tracking. These results emphasize the importance of building
 497 efficient models for embodied agents, to accomplish tasks in dynamic open worlds.
 498

499 4.4 LIMITATION ANALYSIS AND SUMMARY

500 The current RL method shows some capacity to learn spatial-
 501 temporal information and dynamically respond to target move-
 502 ment in most scenarios, but it struggles with executing advanced
 503 actions like bypassing obstacles. In compact Interior cate-
 504 gories and some special environments such as TerrainDemo,
 505 IndustrialArea, and ModularSciFiSeason1, which feature irreg-
 506 ular landscapes, narrow passageways, and maze-like structures,
 507 the agent often collides with casually placed low-level objects.
 508 While the agent can track targets, its insufficient to handle
 509 unpredictable hindrances, especially in key moments like by-
 510 passing corners or tight spaces, which increases the likelihood
 511 of failure. This highlights a significant limitation: although
 512 the agent can learn and react to its environment, it lacks the
 513 higher-level reasoning to anticipate and avoid obstacles effec-
 514 tively. Advanced behaviors like bypassing obstacles are crucial
 515 for improving performance, especially in cluttered environments where basic reactive controls are
 516 insufficient. Incorporating such reasoning mechanisms would help reduce failure rates, particularly
 517 in critical scenarios, and improve overall tracking performance.

518 For the VLM-based method, one key factor contributing to GPT-4o’s notably poor performance,
 519 especially in comparison to the RL methods, is its susceptibility to time delays. From our experience,
 520 this issue becomes particularly evident when the target makes abrupt movements, such as turning
 521 around. Due to the API’s response lag, the GPT-4o system struggles to track the target in real-time,
 522 often losing it before receiving updated instructions. This limitation highlights the difficulty of
 523 real-time processing in embodied tracking tasks using models that rely on slower external API
 524 communications, underscoring the need for more efficient integration methods for such systems.

525 5 CONCLUSIONS

526 In conclusion, we introduce UnrealZoo which offers a versatile platform for advancing embodied
 527 AI research. The diverse, realistic complex environments challenge agents with varying tasks such
 528 as visual navigation, active tracking across various environments, and social tracking in crowds.
 529 The enhanced UnrealCV+ API supports efficient data collection, customization, and task creation,
 530 enabling seamless interaction for both single and multi-agent systems. These features will open
 531 up potential applications like multi-agent rescue missions, collaborative searching, and industrial
 532 automation, making our platform a valuable tool for pushing the boundaries of embodied AI in
 533 real-world scenarios.

534 **Limitations.** While our proposed environment provides diverse and complex scenarios for visual
 535 navigation, tracking, and other visual-based tasks, it currently lacks high-fidelity physical simulation,
 536 limiting the agent’s ability to interact with objects. The interaction between the agent and tiny objects,
 537 such as manipulating objects, is also minimal. Additionally, transferring learned behaviors to different
 538 embodied agents poses a challenge, as adapting models to various physical structures and control
 539 schemes is not yet seamless. These issues highlight areas for further research to enhance interaction
 dynamics and improve generalization across diverse agent embodiments.

500 Table 4: The impact of control fre-
 501 quency on tracking performance.
 502 We evaluate the agent (Offline RL 1
 503 Env.) in the FlexibleRoom environ-
 504 ment using the time dilation wrap-
 505 per to simulate varying control fre-
 506 quencies.

	ER/ EL/ SR.
3 FPS	184/377/0.34
10 FPS	303/449/0.62
30 FPS	368/482/0.92
w/o Control	275/425/0.74

540 REFERENCES
541

- 542 Devendra Singh Chaplot, Dhiraj Gandhi, Saurabh Gupta, Abhinav Gupta, and Ruslan Salakhutdinov. Learning to explore using active neural slam. In *International Conference on Learning Representations*, 2020. URL <https://openreview.net/forum?id=Hk1Xn1BKDH>.
- 543
- 544
- 545 Yuanpei Chen, Yiran Geng, Fangwei Zhong, Jiaming Ji, Jiechuang Jiang, Zongqing Lu, Hao Dong, and Yaodong Yang. Bi-dexhands: Towards human-level bimanual dexterous manipulation. *IEEE Transactions on Pattern Analysis and Machine Intelligence*, 46(5):2804–2818, 2024. doi: 10.1109/TPAMI.2023.3339515.
- 546
- 547
- 548
- 549
- 550 Zhili Cheng, Zhitong Wang, Jinyi Hu, Shengding Hu, An Liu, Yuge Tu, Pengkai Li, Lei Shi, Zhiyuan Liu, and Maosong Sun. Legent: Open platform for embodied agents. *arXiv preprint arXiv:2404.18243*, 2024.
- 551
- 552
- 553 Hai Ci, Mickel Liu, Xuehai Pan, Fangwei Zhong, and Yizhou Wang. Proactive multi-camera collaboration for 3d human pose estimation. In *The Eleventh International Conference on Learning Representations*, 2023. URL <https://openreview.net/forum?id=CPIy9TWFYBG>.
- 554
- 555
- 556 Alexey Dosovitskiy, German Ros, Felipe Codella, Antonio Lopez, and Vladlen Koltun. Carla: An open urban driving simulator. In *Conference on Robot Learning*, pp. 1–16. PMLR, 2017.
- 557
- 558
- 559 Kiana Ehsani, Winson Han, Alvaro Herrasti, Eli VanderBilt, Luca Weihs, Eric Kolve, Aniruddha Kembhavi, and Roozbeh Mottaghi. Manipulathor: A framework for visual object manipulation. In *Proceedings of the IEEE/CVF Conference on Computer Vision and Pattern Recognition*, pp. 4497–4506, 2021.
- 560
- 561
- 562
- 563 Samir Yitzhak Gadre, Kiana Ehsani, Shuran Song, and Roozbeh Mottaghi. Continuous scene representations for embodied ai. In *Proceedings of the IEEE/CVF Conference on Computer Vision and Pattern Recognition*, pp. 14849–14859, 2022.
- 564
- 565
- 566 Adrien Gaidon, Qiao Wang, Yohann Cabon, and Eleonora Vig. Virtual worlds as proxy for multi-object tracking analysis. In *Proceedings of the IEEE Conference on Computer Vision and Pattern Recognition*, pp. 4340–4349, 2016.
- 567
- 568
- 569 Chuang Gan, Jeremy Schwartz, Seth Alter, Damian Mrowca, Martin Schrimpf, James Traer, Julian De Freitas, Jonas Kubilius, Abhishek Bhandwaldar, Nick Haber, Megumi Sano, Kuno Kim, Elias Wang, Michael Lingelbach, Aidan Curtis, Kevin Tyler Feigl, Daniel Bear, Dan Gutfreund, David Daniel Cox, Antonio Torralba, James J. DiCarlo, Joshua B. Tenenbaum, Josh McDermott, and Daniel LK Yamins. ThreeDWorld: A platform for interactive multi-modal physical simulation. In *Thirty-fifth Conference on Neural Information Processing Systems Datasets and Benchmarks Track*, 2021. URL <https://openreview.net/forum?id=db1InWAwW2T>.
- 570
- 571
- 572
- 573
- 574
- 575
- 576
- 577
- 578 Saurabh Gupta, James Davidson, Sergey Levine, Rahul Sukthankar, and Jitendra Malik. Cognitive mapping and planning for visual navigation. In *Proceedings of the IEEE Conference on Computer Vision and Pattern Recognition*, pp. 2616–2625, 2017.
- 579
- 580
- 581 Eric Kolve, Roozbeh Mottaghi, Winson Han, Eli VanderBilt, Luca Weihs, Alvaro Herrasti, Matt Deitke, Kiana Ehsani, Daniel Gordon, Yuke Zhu, et al. AI2-THOR: An interactive 3d environment for visual ai. *arXiv preprint arXiv:1712.05474*, 2017.
- 582
- 583
- 584
- 585 Aviral Kumar, Aurick Zhou, George Tucker, and Sergey Levine. Conservative q-learning for offline reinforcement learning. *Advances in Neural Information Processing Systems*, 33:1179–1191, 2020.
- 586
- 587 Chengshu Li, Ruohan Zhang, Josiah Wong, Cem Gokmen, Sanjana Srivastava, Roberto Martín-Martín, Chen Wang, Gabrael Levine, Michael Lingelbach, Jiankai Sun, et al. Behavior-1k: A benchmark for embodied ai with 1,000 everyday activities and realistic simulation. In *Conference on Robot Learning*, pp. 80–93. PMLR, 2023.
- 588
- 589
- 590
- 591 Yuxing Long, Wenzhe Cai, Hongcheng Wang, Guanqi Zhan, and Hao Dong. Instructnav: Zero-shot system for generic instruction navigation in unexplored environment. In *8th Annual Conference on Robot Learning*, 2024. URL <https://openreview.net/forum?id=fCDOfpTCzZ>.
- 592
- 593

- 594 Wenhan Luo, Peng Sun, Fangwei Zhong, Wei Liu, Tong Zhang, and Yizhou Wang. End-to-end active
 595 object tracking via reinforcement learning. In *International Conference on Machine Learning*, pp.
 596 3286–3295. PMLR, 2018.
- 597 Wenhan Luo, Peng Sun, Fangwei Zhong, Wei Liu, Tong Zhang, and Yizhou Wang. End-to-end active
 598 object tracking and its real-world deployment via reinforcement learning. *IEEE Transactions on*
 599 *Pattern Analysis and Machine Intelligence*, 42(6):1317–1332, 2020. doi: 10.1109/TPAMI.2019.
 600 2899570.
- 601 Guozheng Ma, Lu Li, Sen Zhang, Zixuan Liu, Zhen Wang, Yixin Chen, Li Shen, Xueqian Wang,
 602 and Dacheng Tao. Revisiting plasticity in visual reinforcement learning: Data, modules and
 603 training stages. In *The Twelfth International Conference on Learning Representations*, 2024. URL
 604 <https://openreview.net/forum?id=0aR1s9Yx0L>.
- 605 Volodymyr Mnih, Adria Puigdomenech Badia, Mehdi Mirza, Alex Graves, Timothy Lillicrap, Tim
 606 Harley, David Silver, and Koray Kavukcuoglu. Asynchronous methods for deep reinforcement
 607 learning. In *International Conference on Machine Learning*, pp. 1928–1937, 2016.
- 608 Xavier Puig, Kevin Ra, Marko Boben, Jiaman Li, Tingwu Wang, Sanja Fidler, and Antonio Torralba.
 609 Virtualhome: Simulating household activities via programs. In *Proceedings of the IEEE Conference*
 610 *on Computer Vision and Pattern Recognition*, pp. 8494–8502, 2018.
- 611 Xavier Puig, Eric Undersander, Andrew Szot, Mikael Dallaire Cote, Tsung-Yen Yang, Ruslan Partsey,
 612 Ruta Desai, Alexander Clegg, Michal Hlavac, So Yeon Min, Vladimír Vondruš, Theophile Gervet,
 613 Vincent-Pierre Berges, John M Turner, Oleksandr Maksymets, Zsolt Kira, Mrinal Kalakrishnan,
 614 Jitendra Malik, Devendra Singh Chaplot, Unnat Jain, Dhruv Batra, Akshara Rai, and Roozbeh
 615 Mottaghi. Habitat 3.0: A co-habitat for humans, avatars, and robots. In *The Twelfth International*
 616 *Conference on Learning Representations*, 2024. URL <https://openreview.net/forum?id=4znwzG92CE>.
- 617 Weichao Qiu, Fangwei Zhong, Yi Zhang, Siyuan Qiao, Zihao Xiao, Tae Soo Kim, and Yizhou Wang.
 618 Unrealcv: Virtual worlds for computer vision. In *Proceedings of the 25th ACM International*
 619 *Conference on Multimedia*, pp. 1221–1224, 2017.
- 620 John Schulman, Filip Wolski, Prafulla Dhariwal, Alec Radford, and Oleg Klimov. Proximal policy
 621 optimization algorithms. *arXiv preprint arXiv:1707.06347*, 2017.
- 622 Shital Shah, Debadeepta Dey, Chris Lovett, and Ashish Kapoor. Airsim: High-fidelity visual and
 623 physical simulation for autonomous vehicles. In *Field and Service Robotics*, pp. 621–635, 2018.
- 624 Weiqi Wang, Zihang Zhao, Ziyuan Jiao, Yixin Zhu, Song-Chun Zhu, and Hangxin Liu. Rearrange
 625 indoor scenes for human-robot co-activity. In *2023 IEEE International Conference on Robotics*
 626 *and Automation (ICRA)*, pp. 11943–11949. IEEE, 2023.
- 627 Luca Weihs, Matt Deitke, Aniruddha Kembhavi, and Roozbeh Mottaghi. Visual room rearrangement.
 628 In *Proceedings of the IEEE/CVF Conference on Computer Vision and Pattern Recognition*, pp.
 629 5922–5931, 2021.
- 630 Yi Wu, Yuxin Wu, Georgia Gkioxari, and Yuandong Tian. Building generalizable agents with a
 631 realistic and rich 3d environment. *arXiv preprint arXiv:1801.02209*, 2018.
- 632 Fei Xia, Amir R Zamir, Zhiyang He, Alexander Sax, Jitendra Malik, and Silvio Savarese. Gibson env:
 633 Real-world perception for embodied agents. In *Proceedings of the IEEE Conference on Computer*
 634 *Vision and Pattern Recognition*, pp. 9068–9079, 2018.
- 635 Guowei Xu, Ruijie Zheng, Yongyuan Liang, Xiyao Wang, Zhecheng Yuan, Tianying Ji, Yu Luo,
 636 Xiaoyu Liu, Jiaxin Yuan, Pu Hua, Shuzhen Li, Yanjie Ze, Hal Daumé III, Furong Huang, and
 637 Huazhe Xu. Drm: Mastering visual reinforcement learning through dormant ratio minimization.
 638 In *The Twelfth International Conference on Learning Representations*, 2024. URL <https://openreview.net/forum?id=MSe8YFbhUE>.
- 639 Karmesh Yadav, Ram Ramrakhya, Arjun Majumdar, Vincent-Pierre Berges, Sachit Kuhar, Dhruv
 640 Batra, Alexei Baevski, and Oleksandr Maksymets. Offline visual representation learning for
 641 embodied navigation. In *Workshop on Reincarnating Reinforcement Learning at ICLR 2023*, 2023.

- 648 Jihan Yang, Runyu Ding, Ellis Brown, Xiaojuan Qi, and Saining Xie. V-irl: Grounding virtual
 649 intelligence in real life. *arXiv preprint arXiv:2402.03310*, 2024.
- 650
- 651 Jinyu Yang, Mingqi Gao, Zhe Li, Shang Gao, Fangjing Wang, and Feng Zheng. Track anything:
 652 Segment anything meets videos. *arXiv preprint arXiv:2304.11968*, 2023.
- 653 Naoki Yokoyama, Sehoon Ha, Dhruv Batra, Jiuguang Wang, and Bernadette Bucher. Vlfm: Vision-
 654 language frontier maps for zero-shot semantic navigation. In *International Conference on Robotics*
 655 and *Automation (ICRA)*, 2024.
- 656
- 657 Tianhe Yu, Deirdre Quillen, Zhanpeng He, Ryan Julian, Karol Hausman, Chelsea Finn, and Sergey
 658 Levine. Meta-world: A benchmark and evaluation for multi-task and meta reinforcement learning.
 659 In *Conference on Robot Learning*, pp. 1094–1100. PMLR, 2020.
- 660 Zhecheng Yuan, Zhengrong Xue, Bo Yuan, Xueqian Wang, Yi Wu, Yang Gao, and Huazhe Xu.
 661 Pre-trained image encoder for generalizable visual reinforcement learning. In *Advances in Neural*
 662 *Information Processing Systems*, volume 35, pp. 13022–13037, 2022.
- 663
- 664 Jiazhao Zhang, Kunyu Wang, Rongtao Xu, Gengze Zhou, Yicong Hong, Xiaomeng Fang, Qi Wu,
 665 Zhizheng Zhang, and Wang He. Navid: Video-based vlm plans the next step for vision-and-
 666 language navigation. *arXiv preprint arXiv:2402.15852*, 2024.
- 667
- 668 Fangwei Zhong, Peng Sun, Wenhan Luo, Tingyun Yan, and Yizhou Wang. AD-VAT: An asymmetric
 669 dueling mechanism for learning visual active tracking. In *International Conference on Learning*
Representations, 2019. URL <https://openreview.net/forum?id=HkgYmhR9KX>.
- 670
- 671 Fangwei Zhong, Peng Sun, Wenhan Luo, Tingyun Yan, and Yizhou Wang. Towards distraction-robust
 672 active visual tracking. In *International Conference on Machine Learning*, pp. 12782–12792.
 673 PMLR, 2021.
- 674
- 675 Fangwei Zhong, Xiao Bi, Yudi Zhang, Wei Zhang, and Yizhou Wang. Rspt: reconstruct surround-
 676 ings and predict trajectory for generalizable active object tracking. In *Proceedings of the AAAI*
Conference on Artificial Intelligence, volume 37, pp. 3705–3714, 2023.
- 677
- 678 Fangwei Zhong, Kui Wu, Hai Ci, Churan Wang, and Hao Chen. Empowering embodied visual
 679 tracking with visual foundation models and offline rl. *arXiv preprint arXiv:2404.09857*, 2024.
- 680
- 681 Gengze Zhou, Yicong Hong, and Qi Wu. Navgpt: Explicit reasoning in vision-and-language
 682 navigation with large language models. In *Proceedings of the AAAI Conference on Artificial*
Intelligence, volume 38, pp. 7641–7649, 2024a.
- 683
- 684 Qinhong Zhou, Sunli Chen, Yisong Wang, Haozhe Xu, Weihua Du, Hongxin Zhang, Yilun Du,
 685 Joshua B. Tenenbaum, and Chuang Gan. HAZARD challenge: Embodied decision making
 686 in dynamically changing environments. In *The Twelfth International Conference on Learning*
Representations, 2024b. URL <https://openreview.net/forum?id=n6mLhaBahJ>.
- 687
- 688 Yuke Zhu, Roozbeh Mottaghi, Eric Kolve, Joseph J. Lim, Abhinav Gupta, Li Fei-Fei, and Ali
 689 Farhadi. Target-driven visual navigation in indoor scenes using deep reinforcement learning. In
 690 *International Conference on Robotics and Automation (ICRA)*, 2017.
- 691
- 692
- 693
- 694
- 695
- 696
- 697
- 698
- 699
- 700
- 701

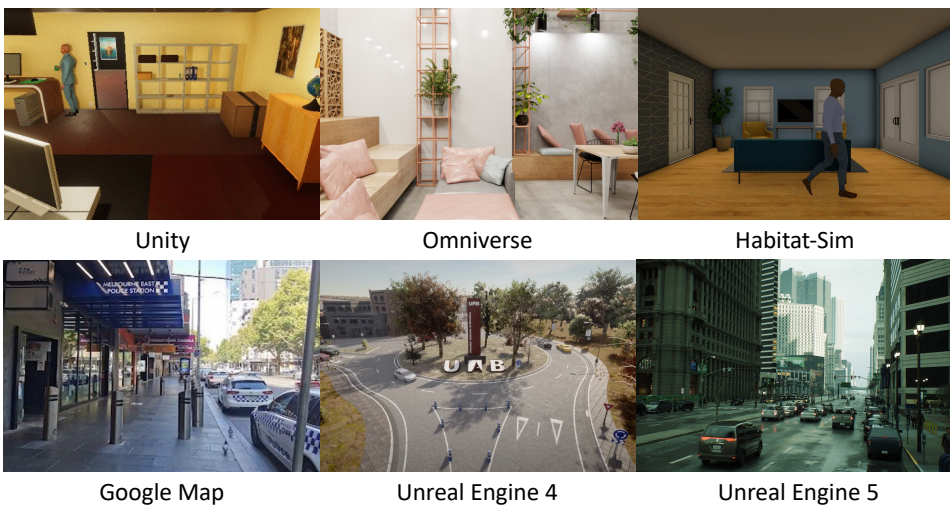
702 A UE ENVIRONMENTS

704 A.1 COMPARISON WITH OTHER SIMULATORS

706 To better explain Table 1, we list the description of each symbol about the scene types and playable
 707 entities in Table 6. Since photorealism mainly relies on the engine used, we visualize the snapshots
 708 rendered by different engines in Figure 6. Note that Google Maps are images captured in the
 709 real world, but can not simulate the dynamic of the scenes and interactions between objects. By
 710 utilizing advanced rendering and physics engines, Unreal Engine simulates large-scale photorealistic
 711 environments that are not only visually appealing but also capable of complex interactions between
 712 agents and objects. So we choose to build environments on Unreal Engine.

713 Table 6: The description of symbols used in Table 1.

715 Symbol	716 Description
716	716 Scenes with indoor furnishings
717	717 Scenes with outdoor roads
718	718 Natural landscapes with trees of varying heights and grasslands
719	719 Buildings with castle-style architecture
720	720 Realistic construction site scenes with a variety of construction tools and equipment
721	721 Realistic factory scenes with internal roads and factory facilities
722	722 Scenes with residential community settings
723	723 Scenes featuring temple architecture with stairs, lofts, and shrines
724	724 Sports venue scenes
725	725 Common urban public transportation station scenes
726	726 Hospital interior scenes with detailed elements
727	727 High-fidelity urban environments
728	728 Scenes with a desert and seaside landscape style
729	729 Human agents with detailed features such as hair textures, clothing, and actions
730	730 Mobile robot
731	731 Driveable car
732	732 Animal agents, including common animal species such as cats, dogs, lions, tigers, etc.
733	733 Driveable motorbike
734	734 Drones
735	735 Virtual camera that has no physical entity and is movable



752 Figure 6: Comparison of the visual realism of different engines: we show the snapshots captured
 753 from different engines to compare the photo-realism of different environments for an intuitive feeling.
 754 Note that Google Maps capture and reconstruct the images from the real world, but can not simulate
 755 the dynamic of the scenes and interactions between agents and objects.



Figure 7: Two photo-realistic environments used for visual navigation.

A.2 ENVIRONMENTS USED IN VISUAL NAVIGATION

We carefully selected two photo-realistic environments (**Roof** and **Factory**) for training and evaluating navigation in the wild, shown in Figure 7. The Roof environment features multiple levels connected by staircases and large pipelines scattered on the ground, providing an ideal setting for the agent to learn complex action combinations for transitioning between levels, such as jumping, climbing, and navigating around obstacles. The Factory environment, on the other hand, is characterized by compact boxes and narrow pathways, challenging the agent to determine the appropriate moments to jump over obstacles or crouch to navigate under them. These two environments offer diverse spatial structures, enabling agents to develop an understanding of multi-level transitions and precise obstacle avoidance.

A.3 ENVIRONMENTS USED IN ACTIVE VISUAL TRACKING

For training agents via offline reinforcement learning, we selected 8 distinct environments to collect demonstrations, as is shown in Figure 10. To comprehensively evaluate the generalization of the active visual tracking agents, we selected **16** distinct environments, categorized into Interior Scenes, Palaces, Wilds, and Modern Scenes. Each category presents unique challenges: 1) **Interior Scenes** feature complex indoor structures with frequent obstacles; 2) **Palaces** include multi-level structures and narrow pathways; 3) **Wilds** encompass irregular terrain and varying illumination; 4) **Modern Scenes** offer high-fidelity, real-world scenarios with modern buildings and objects. These diverse environments facilitate a thorough assessment of the agent’s generalization capabilities across varying complexities. The snapshot of each environment is shown in Figure 8.

A.4 NAVIGATION MESH

Based on NavMesh, we build an internal navigation system, allowing agents to autonomously navigate with the built-in AI controller in the Unreal Engine. This includes path-finding and obstacle-avoidance capabilities, ensuring smooth and realistic movement throughout diverse terrains and structures. Moreover, in our City style map, we manually construct road segmentation, we manually segment the roads to distinguish between pedestrian and vehicle pathways. When agents use the navigation system for autonomous control, they will navigate the shortest path based on the priority of the different areas. Figure 9 shows an example of the rendered semantic segmentation for NavMesh in an urban city.

B EXEMPLAR TASKS

B.1 VISUAL NAVIGATION

In this task, the agent is initialized at a random location in the environment at the beginning of each episode, while the target object’s location and category remain fixed throughout. The agent must rely on its first-person view observations and the relative spatial position of the target as input. The

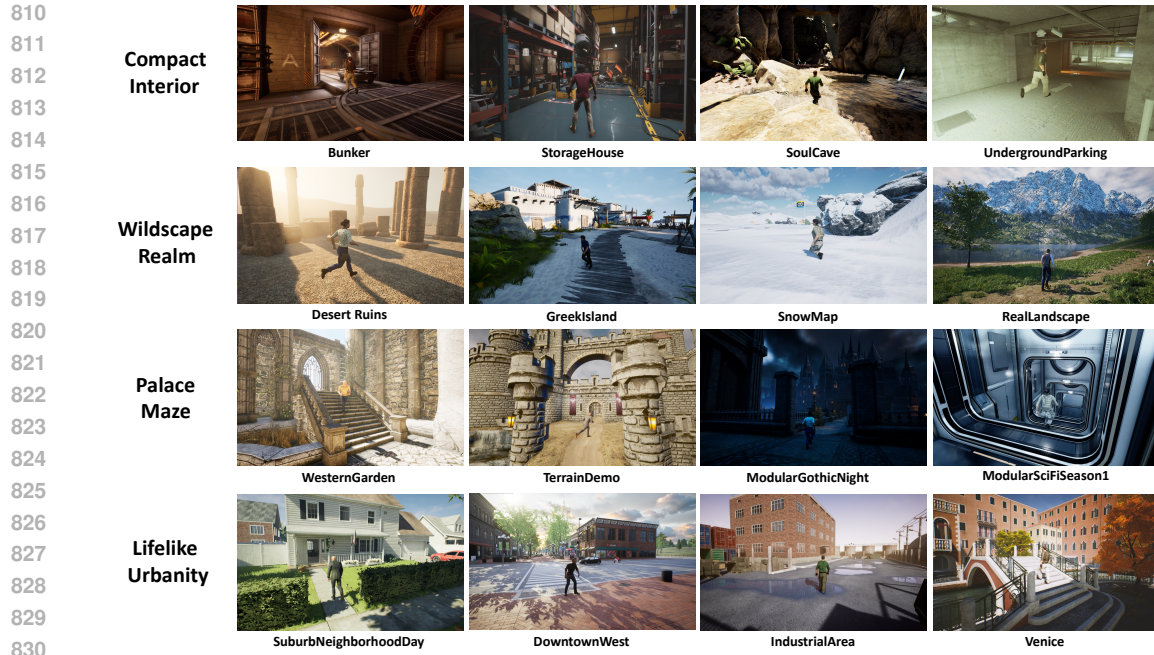


Figure 8: The snapshots of 16 environments used for testing active visual tracking agents. The text on the left indicates the category corresponding to that line of environment.



Figure 9: An example of the NavMesh with semantic segmentation. The human character will prioritize using the pink area for pedestrian navigation tasks, while the vehicles will use the blue area.

ultimate objective is to locate the target object within 2000 steps. Success is defined by the agent reducing the relative distance to less than 3 meters and aligning its orientation such that the relative rotation between the target and the agent is smaller than 30 degrees (in the front of the agent). This setup challenges the agent to optimize its movements and decision-making while adapting to the randomized starting conditions and dynamic environment. All methods in the task share the same discrete action space to control the movement, consisting of moving forward (+1 meter/s), moving backward (-1 meter/s), turning left (-15 degrees/s), turning right (+15 degrees/s), jumping (two

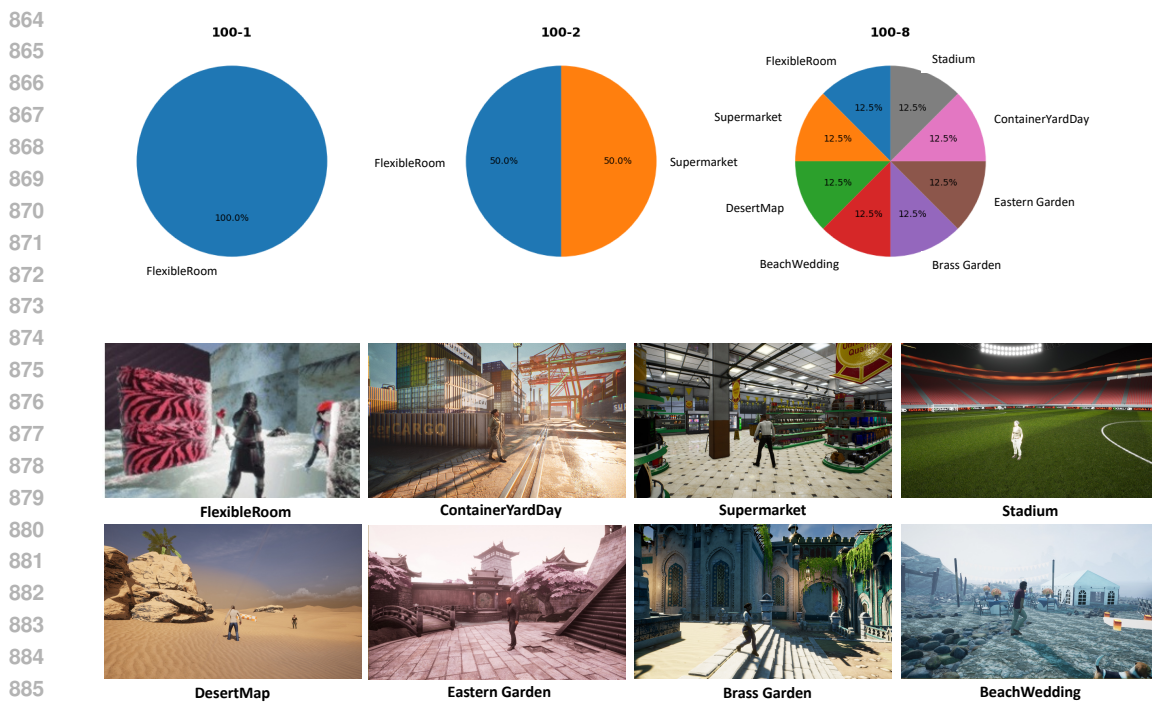


Figure 10: The 8 environments used for collecting offline dataset.

continuous jumping actions trigger the climbing action), crouching, and holding position. This action space enables the agent to navigate and interact with complex 3D environments, making strategic decisions in real-time to reach the target object efficiently. The step reward for the agent is defined as:

$$r(t) = \tanh\left(\frac{\text{dis2target}(t-1) - \text{dis2target}(t)}{\max(\text{dis2target}(t-1), 300)} - \frac{|\text{Ori}|}{90^\circ}\right) \quad (1)$$

where $\text{dis2target}(t)$ is the Euclidean distance between the agent and the target at a given timestep t and $|\text{Ori}|$ is the absolute orientation error (in degrees) between the agent’s current heading and the direction toward the target, normalized by 90°

B.2 ACTIVE VISUAL TRACKING

Referring to previous works (Zhong et al., 2024), we use human characters as an agent player and a continuous action space for agents. The action space contains two variables: the angular velocity and the linear velocity. Angular velocity varies between $-30^\circ/s$ and $30^\circ/s$, while linear velocity ranges from $-1 m/s$ to $1 m/s$. In the agent-centric coordinate system, the reward function is defined as:

$$r = 1 - \frac{|\rho - \rho^*|}{\rho_{\max}} - \frac{|\theta - \theta^*|}{\theta_{\max}} \quad (2)$$

where (ρ, θ) denotes the current target position relative to the tracker, $(\rho^*, \theta^*) = (2.5m, 0)$ represents the expected target position, i.e., the target should be $2.5m$ in front of the tracker. The error is normalized by the field of the view $(\rho_{\max}, \theta_{\max})$. During execution, an episode ends with a maximum length of 500 steps, applying the appropriate termination conditions. In the experiment, we adopt the original neural network structure and parameters, as listed in Table 9 and 10.

B.3 TASK CONFIGURATION IN A JSON FILE

We provide an example of the task configuration JSON file in Figure 11. Using the JSON file, we can easily set the configuration of the binary, the continuous and discrete action space for each agent, the placement of the binding camera, choose the area to reset, and other hyper-parameters about the environments.

918 **A Json File for Task Configuration**

```

919
920     "env_name": env_name,
921     "env_bin": path-to-binary,
922     "env_map": map_name,
923     "env_bin_win": path-to-binary(for windows),
924     "third_cam": {"cam_id": 0,"pitch": -90,"yaw": 0,"roll": 0,"height_top_view": 1460.0,"fov": 90},
925     "height": 460.0,
926     "interval": 1000,
927     "agents": {
928         "player": {
929             "name": ["BP_Character_923"],
930             "cam_id": [3],
931             "class_name": ["bp_character_C"],
932             "internal_nav": true,
933             "scale": [1,1,1],
934             "relative_location": [20,0,0],
935             "relative_rotation": [0,0,0],
936             "head_action_continuous": {"high": [15,15,15], "low": [-15,-15,-15]},
937             "head_action": [[0,0,0],[0,30,0],[0,-30,0]],
938             "animation_action": ["stand","jump","crouch"],
939             "move_action": [
940                 [angular, velocity]
941                 ...
942             ],
943             "move_action_continuous": {"high": [30,100],"low": [-30,-100]}
944         },
945         "animal": {
946             "name": ["BP_animal_2"],
947             "cam_id": [1],
948             "class_name": ["BP_animal_C"],
949             "internal_nav": true,
950             "scale": [1,1,1],
951             "relative_location": [20,0,0],
952             "relative_rotation": [0,0,0],
953             "move_action": [
954                 [angular, velocity]
955                 ...
956             ],
957             "move_action_continuous": {"high": [30,100],"low": [-30,-100]}
958         },
959         "drone": {
960             "name": ["BP_Drone01_2"],
961             "cam_id": [2],
962             "class_name": ["BP_drone01_C"],
963             "internal_nav": false,
964             "scale": [0.1,0.1,0.1],
965             "relative_location": [0,0,0],
966             "relative_rotation": [0,0,0],
967             "move_action": [
968                 [angular, velocity]
969                 ...
970             ],
971             "move_action_continuous": {"high": [1,1,1,1],"low": [-1,-1,-1,-1]}
972         }
973     },
974     "safe_start": [
975         [x,y,z],
976         ...
977     ],
978     "reset_area": [x_min,x_maxin,y_min,y_max,z_min,z_max],
979     "random_init": false,
980     "env": {"interactive_door": []},
981     "obj_num": 466,
982     "size": 192555.0,
983     "area": 9900.0,
984     "bbox": [110.0, 90.0, 19.45]
985 
```

Figure 11: An example of the task configuration file in JSON format.

B.4 COLLECTING DEMONSTRATION FOR ACTIVE VISUAL TRACKING

To demonstrate the flexibility of the environment, we use state-based expert policy and the multi-level perturbation strategy (Zhong et al., 2024) to automatically generate various imperfect demonstrations

as the offline dataset. For active visual tracking, we employ three distinct datasets for training agents via offline reinforcement learning (Offline RL) algorithms, referred to as *1 Env.*, *2 Envs.*, and *8 Envs.*. The detailed composition of each dataset is depicted in Figure 10. For the *1 Env.* dataset, we use only the FlexibleRoom, an abstract environment enriched with diverse augmentation factors, to gather 100k steps of trajectory data. For *2 Envs.*, we collect 50k step trajectories from FlexibleRoom and an additional 50k steps from the Supermarket environment. The *8 Envs.* dataset involves eight different environments, with 12.5k steps collected from each. Therefore, **the total amount of data in the three datasets is the same (100k) to ensure the fairness of the comparison.** These dataset configurations aim to highlight the critical role of environment diversity in enhancing the generalization capabilities of embodied AI agents.

C IMPLEMENTATION DETAILS OF AGENTS

C.1 RL-BASED AGENTS

Learning to navigate with online reinforcement learning. For navigation, we construct an RL-based end-to-end model, using A3C (Mnih et al., 2016) to accelerate online reinforcement learning in a distributed manner. The model’s structure is as follows: a mask encoder extracts spatial visual features from the segmentation mask, which are then passed to a temporal encoder to capture latent temporal information. Finally, the spatiotemporal features, concatenated with the target’s relative spatial position, are fed into the actor-critic network to optimize the actor layer for action prediction. The detailed network structure and parameters used in the experiment are listed in Table 7 and 8. Here, we provide the training curves in *Roof* and *Factory* environments, depicted in Figure 15. In the *Factory*, we set the number of workers to 4, while in the *Roof*, the number of workers is set to 6. It can be observed that, for Online RL, the number of workers and the complexity of environments have a significant impact on training efficiency. Looking forward, we anticipate that offline-based algorithms can effectively address the challenges of training efficiency and generalization.

Table 7: Details the neural network structure of RL-based agent for navigation task, where $5 \times 5\text{-}32S1$ means 32 filters of size 5×5 and stride 1, FC256 indicates the fully connected layer with output dimension 256, and LSTM128 indicates that all the sizes in the LSTM unit are 128.

Mask Encoder								
Layer#	CNN	Pool	CNN	Pool	CNN	Pool	CNN	Pool
Parameters	$5 \times 5\text{-}32S1$	2-S2	$5 \times 5\text{-}32S1$	2-S2	$4 \times 4\text{-}64S1$	2-S2	$3 \times 3\text{-}64S1$	2-S2
Module	Temporal Encoder		Actor			Critic		
Layer#	FC	LSTM	FC			FC		
Parameters	256	128	2			2		

Table 8: The experiment setting and hyper-parameters used for training the RL-based navigation agent.

Name	Value	Name	Value
Learning Rate	1e-4	LSTM update step	20
workers (Roof)	6	LSTM Input Dimension	256
workers (Factory)	4	LSTM Output Dimension	128
Position Input Dimension	2	LSTM Hidden Layer size	1

Learning to track with offline reinforcement learning. For the tracking task, we adopt an offline reinforcement learning (Offline RL) approach to enhance training efficiency and improve the agent’s generalization to unknown environments. Specifically, we build an end-to-end model trained using offline data and the conservative Q-learning (CQL) strategy (Kumar et al., 2020). We adopt the same model structure from the latest visual tracking agent (Zhong et al., 2024), consisting of a Mask Encoder, a Temporal Encoder, and an Actor-Critic network. Detailed model structures and training parameters are summarized in Table 9 and 10. Additionally, we provide the model’s loss curves under different dataset setups, as shown in Figure 14. The model achieves near-convergence within

two hours across all dataset setups. To ensure the loss curves stabilize fully, we continued training for an additional three hours, during which no significant further decrease in the loss was observed. A comprehensive evaluation of the model’s performance is presented in Tables 11 and 12, highlighting its strong generalization to unseen environments and robustness to dynamic disturbances. The training efficiency, generalization capability, and robustness achieved by offline RL further reinforce our belief that offline RL methods will become a mainstream approach for rapid prototyping and iteration in embodied intelligence systems.

Table 9: Network structure used in the offline RL method (Zhong et al., 2024), where $8 \times 8\text{-}16S4$ means 16 filters of size 8×8 and stride 4, FC256 indicates a fully connected layer with dimension 256, and LSTM64 indicates that all sizes in the LSTM unit are 64.

Module	Mask Encoder			Temporal Encoder	Actor	Critic
Layer#	CNN	CNN	FC	LSTM	FC	FC
Parameters	$8 \times 8\text{-}16S4$	$4 \times 4\text{-}32S2$	256	64	2	2

Table 10: The hyper-parameters used for offline training and the policy network.

Name	Value	Name	Value
Learning Rate	3e-5	LSTM update step	20
Discount Factor	0.99	LSTM Input Dimension	256
Batch Size	32	LSTM Output Dimension	64
LSTM Hidden Layer size	1		

C.2 VLM-BASED AGENTS

We built agents with a reasoning framework based on the Large Vision-Language Model. We employ OpenAI GPT-4o as the base model. System prompt used in the navigation task, as shown in Figure 13 and system prompt used in the tracking task, as shown in Figure 12.

C.3 HUMAN BENCHMARK FOR NAVIGATION

In the navigation task, we incorporated human evaluation as a baseline for comparison to demonstrate the existing gap between the current method and optimal navigation performance. Specifically, **five male and five female** evaluators participated in the assessment, performing the same navigation tasks under comparable conditions.

Before each human evaluator began their assessment, we provided a free-roaming perspective to familiarize them with the map structure and clearly conveyed the target’s location and image. This ensured that human evaluators had a comprehensive understanding of the environment and the target’s position. During the evaluation, the player was randomly initialized in the environment, and human evaluators used the keyboard to control the agent’s movements. Each human evaluator repeated the experiment five times, providing multiple data points to ensure reliability and reduce variability in performance measurements. The termination conditions for the evaluation were identical to those applied to the RL-based agent, ensuring consistency in the comparison.

1080
1081
1082
1083
1084

1085
1086

System Prompt used for active tracking

1087
1088
1089
1090

Objective:

You are an intelligent tracking agent designed to control the robot to track the person in the view. The first person in your view is your target. You need to provide concrete moving strategies to help robot tracking the target in the given environment.

1091
1092
1093
1094
1095
1096
1097
1098
1099
1100
1101

Representation details:

1. Moving instructions are concrete actions that the robot can take to adjust its viewpoint and distance to the target. The moving instructions include:
 - move closer: Move the robot closer to the target. This should be chosen when the target is too far away from the robot and there is no obstacle in the way.
 - move further: Move the robot further away from the target. This should be chosen when the target is too close to the robot and only part of the target body is visible in the view.
 - keep current: Maintain the current distance and angle between the robot and the target. This is chosen when the target is fully observable in the view and there is enough space in front of both tracker and target without any potential obstacles that may cause collision and occlusion.
 - turn left: Turn the robot to left direction, the target will move towards the right side in next frame.
 - turn right: Turn the robot to right direction, the target will move towards the left side in next frame.

1102
1103
1104

Input Understanding:

1. **Image:** We provide a first-person view observation of the robot to help you understand the surrounding environment. The observation is represented as a color image from the tracker's first-person perspective.

1105
1106
1107
1108

Output Understanding:

1. **Moving Strategy:** A temporal reasonable move strategy to adjust the robot viewpoint and distance to achieve robot's long-term tracking task. This should be represented as a concrete moving instructions, the instructions should be chosen from "move closer", "move further", "keep current", "turn left", "turn right". Format - [Keep current].

1109
1110
1111
1112
1113
1114
1115
1116
1117
1118
1119
1120
1121
1122
1123
1124
1125
1126

Strategy Considerations:

1. If the person's horizontal position in the robot's field of view deviates from the center by more than 25% of the image width, we consider the target to be on one side of the image, otherwise we say the target is near the center.
2. To provide a reasonable moving strategy, you should think step by step based on the input image and the following hints:
 - 1) If the person is too close to the robot and the target in the image is clipped, robot should move further first to obtain a better view.
 - 2) If the person's size in the view is too small in the image, robot should move closer to obtain a better view.
 - 3) If the person may be occluded by obstacles or structures in the future, the robot should move closer to avoid losing the person in the next frame.
 - 4) If the person is near the right edge in the image and there is no immediate obstacle in front of the robot, the robot should turn right to keep the person near the center in the image.
 - 5) If there is an immediate hinder obstacle in front of the robot, turn right or left to a clean space first.
 - 6) If there is any potential occlusion effect or obstacles on either side of the person's walking path, the robot should move closer to avoid losing the person in the next frame.
 - 7) If there is no person in the current image, turn right or turn left to search the person.

1127
1128
1129
1130
1131
1132
1133

Figure 12: System prompt used for tracking.

1134
 1135 **System Prompt used for navigation**

1136 **Objective:**
 1137 You are an intelligent navigation agent designed to control the robot to navigate to
 the target object location based on first-person observation and provide a
 1138 relative position between the robot and the target. You need to provide an action
 1139 sequence to help the robot move to the target location.

1140 **Representation details:**
 1141 1. Relative Position: This contains three elements, in the format - [Distance,
 Direction, Height].
 1142 -**Distance**: The relative distance between the robot and the target object.
 1143 -**Direction**: The target object's relative direction to the robot, represented in
 degrees. \
 1144 A positive value represent the target is on the right side of the robot
 with corresponding angle and a negative value represent the target is
 on the left side of the robot with corresponding angle. \
 1145 The absolute value of the angle larger than 90 degree means the target is
 behind the robot. \
 1146 -**Height**: The relative vertical position, where a positive value indicates that the
 target is higher than the robot.

1147 1. Actions: These are the movements the robot can perform to adjust its position. The
 available actions include:
 1148 -Move Forward: Propel the robot forward by 100 centimeter.
 1149 -Move Backward: Propel the robot backward by 100 centimeter.
 1150 -Turn Left: Rotate the robot 15 degrees to the left.
 1151 -Turn Right: Rotate the robot 15 degrees to the right.
 1152 -Jump: Make the robot leap into the air, robot should use this action to jump over
 obstacles or climb over stairs.
 1153 -Crouch: Lower the robot into a crouching position for 2 seconds, after which it
 will automatically stand up.
 1154 -Keep Current: Maintain the robot's current position without any movement.

1155
 1156 **Input Understanding:**
 1157 1.**Image:** We provide a first-person view observation of the robot to help you
 understand the surrounding environment. The observation is represented as a color
 image from the robot's first-person perspective.
 1158 2.**Relative Position:** This data provides the target object's relative position to
 the robot, including the distance, direction, and height. The distance is measured
 in centimeters, the direction in degrees, and the height in centimeters.

1159 **Output Understanding:**
 1160 1. **Action Sequence:** This is a series of Three continuous actions that the robot
 should take to navigate toward the target object. Each sequence must consider the
 provided relative position data and the first-person observation. \
 1161 The actions should be ordered logically to effectively move the
 robot closer to the target, adjusting its direction,
 distance, and height as needed. \
 1162 The action sequence should be clear and executable, enabling
 the robot to reach the target efficiently while avoiding
 obstacles and maintaining stability
 1163 in the format - [Action1, Action2, Action3]. Each action should
 be choose from the available actions mentioned above.

1164
 1165 **Strategy Considerations:**
 1166 1.Assessing Relative Position: Begin by evaluating the target object's relative
 position in terms of distance, direction, and height to inform the action sequence
 .
 1167 2.Action Combination for Navigation: Utilize the action sequence to create effective
 combinations, each action will last for 1 seconds. For example:
 1168 -Consider using multiple consecutive actions like [Move Forward, Jump, Jump] to
 climb over the front obstacles or boxes.
 1169 -Consider using [Move Backward, Move Backward, Move Backward] to move the robot
 avoid a front wall or fence.
 1170 3.Obstacle Detection: Leverage the first-person observation to identify obstacles.
 1171 Based on their location, formulate action sequences that facilitate smooth
 navigation while avoiding collisions.
 1172 4.Efficient Pathing: Ensure the action sequence is designed to dynamically adjust the
 robot movement toward target object, which is minimize the distance and direction
 value in **Relative Position**.
 1173 5.Sequence Validation: Validate the generated action sequence and consider past
 memories to ensure it is practical given the current environment and obstacles,
 making long-term adjustments as necessary.

1174 **Instructions:**
 1175 1.Provide ONLY the action sequence in the [output:] strictly following the format -[
 Action1, Action2, Action3], without additional explanations or additional text.

Figure 13: System prompt used for navigation.



Figure 14: The CQL loss curve during offline training with different offline datasets.

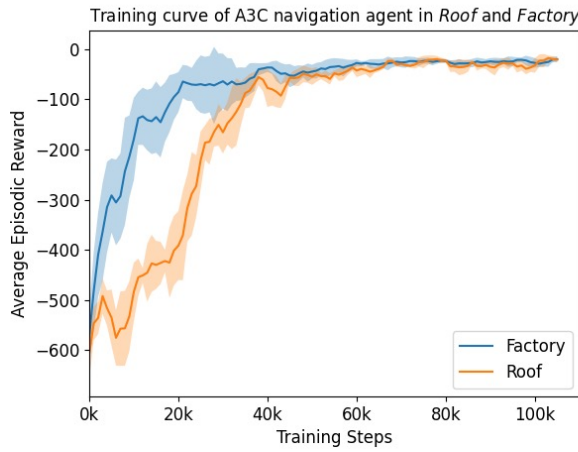


Figure 15: The learning curves for RL-based navigation agent in two environments: Roof and Factory. We use A3C (Mnih et al., 2016) to learn the navigation policy via trial-and-error interactions. In the Factory (blue line plot), the number of asynchronous workers is set to 4, while in the Roof environment (orange line plot), the number of asynchronous workers is set to 6.

D ADDITIONAL RESULTS

D.1 LEARNING CURVE

We provide the CQL loss curve under the *1 Env.*, *4 Envs.* and *8 Envs.* training setup. As shown in Figure 14, the offline model approaches convergence after two hours and we continued training for another three hours after nearing convergence, observing no significant further decrease in the loss. Note that the offline training was conducted on a Nvidia RTX 4090 GPU.

D.2 EVALUATE TRACKING AGENTS ACROSS 16 UNSEEN ENVIRONMENTS

We provide the detailed quantitative evaluation results (episodic returns, episode length, success rate) of the RL-based embodied tracking agents across 16 environments, listed in Table 11. In each environment, we report the average results over 50 episodes. The results show that in the *Palace Maze*, which contains abundant structural obstacles, the agent’s tracking performance was generally weaker compared to the other three categories. In contrast, the agent performed generally better in *Lifelike Urbanity*, characterized by its relatively regular and flat terrain. Additionally, we observed that as the diversity of the training environments increased, the agent’s tracking performance improved across all four environment categories. This highlights the positive impact of diverse training data on enhancing the agent’s overall tracking effectiveness. We also provide vivid demo videos in <https://unrealzoo.notion.site/task-evt>.

Table 11: Quantitative evaluation results of the offline RL method across 16 environments. The environments are grouped into four categories: Compact Interior, Wildscape Realm, Palace Maze, and Lifelike Urbanity. The table compares the performance of agents trained on different offline dataset settings: 1 Env. (single environment), 2 Envs. (two environments), and 8 Envs. (eight environments). Each cell presents three metrics from left to right: Average Episodic Return (ER), Average Episode Length (EL), and Success Rate (SR).

Category	Environment Name	1 Env.	2 Envs.	8 Envs.
		ER/EL/SR	ER/EL/SR	ER/EL/SR
Compact Interior	Bunker	241/412/0.56	245/391/0.56	234/429/0.70
	StorageHouse	213 /424 /0.68	275/449/0.76	170/434/0.64
	SoulCave	229/402/0.60	252/422/0.56	206/405/0.58
	UndergroundParking	179/391/0.56	250/424/0.62	184/410/0.60
Wildscape Realm	Desert Ruins	209/392/0.54	293/449/0.70	277/453/0.70
	GreekIsland	245/411/0.62	264/423/0.64	257/466/0.78
	SnowMap	204/399/0.62	322/456/0.78	278/474/0.86
	RealLandscape	171 /383/0.42	225/372/0.44	223/444/0.70
Palace Maze	WesternGarden	230/403/0.54	209/408/0.54	296/472/0.82
	TerrainDemo	232/411/0.56	233/403/0.56	192/411/0.56
	ModularGothicNight	190/360/0.52	244/423/0.62	272/456/0.76
	ModularSciFiSeason1	168/365/0.42	172/354/0.42	211/393/0.48
Lifelike Urbanity	SuburbNeighborhoodDay	224/422/0.64	328/457/0.72	242/457/0.76
	DowntownWest	296/460/0.78	317/456/0.76	292/469/0.86
	Factory	278/434/0.64	291/452/0.74	249/435/0.64
	Venice	295/441/0.70	323/448/0.82	294/474/0.84

Table 12: Quantitative evaluation results of the tracking agents across 4 different category environments with **4 distractors (4D)**, **8 distractors (8D)**, and **10 distractors (10D)** respectively. The table compares the performance of agents trained on different offline dataset settings: 1 Env. (single environment), 2 Envs. (two environments), and 8 Envs. (eight environments). Each cell presents three metrics from left to right: Average Episodic Return (ER), Average Episode Length (EL), and Success Rate (SR).

Category	Environment Name	1 Env.	2 Envs.	8 Envs.
		ER/EL/SR	ER/EL/SR	ER/EL/SR
Compact Interior	StorageHouse (4D)	117/343/0.40	181/375/0.52	190/428/0.62
	StorageHouse (8D)	143/341/0.34	151/338/0.44	165/366/0.49
	StorageHouse (10D)	81/324/0.36	109/331/0.42	107/357/0.50
Wildscape Realm	DesertRuins (4D)	317/469/0.72	333/456/0.70	354/466/0.74
	DesertRuins (8D)	213/406/0.50	316/445/0.58	267/444/0.68
	DesertRuins (10D)	188/390/0.44	252/382/0.50	253/447/0.64
Palace Maze	TerrainDemo (4D)	221/398/0.44	286/454/0.65	312/460/0.77
	TerrainDemo (8D)	211/384/0.39	239/412/0.49	252/420/0.52
	TerrainDemo (10D)	189/377/0.36	232/404/0.48	224/429/0.66
Lifelike Urbanity	SuburbNeighborhoodDay (4D)	192/407/0.46	256/381/0.50	265/392/0.60
	SuburbNeighborhoodDay (8D)	131/325/0.36	229/369/0.48	247/385/0.56
	SuburbNeighborhoodDay (10D)	162/355/0.44	180/340/0.40	165/376/0.44

D.3 EVALUATE TRACKING AGENTS ACROSS UNSEEN SOCIAL ENVIRONMENTS

We select 4 environments from different categories as the testing environments, including StorageHouse, DesertRuins, TerrainDemo, and SurburNeighborhoodDay. We test the distraction robustness of the social tracking agents by adding different numbers of distractors (4, 8, 10) in the environment. The distractors randomly walk around the environment, which may produce various unexpected

1296 perturbations to the tracker, such as visual distractions, occlusion, or blocking the tracker’s path. As
1297 shown in Table 12, the tracking performance of the three agents steadily decays with the increasing
1298 number of distractors.
1299
1300
1301
1302
1303
1304
1305
1306
1307
1308
1309
1310
1311
1312
1313
1314
1315
1316
1317
1318
1319
1320
1321
1322
1323
1324
1325
1326
1327
1328
1329
1330
1331
1332
1333
1334
1335
1336
1337
1338
1339
1340
1341
1342
1343
1344
1345
1346
1346
1347
1348
1349